J Acupunct Meridian Stud 2015;8(6):294—300

Available online at www.sciencedirect.com

Journal of Acupuncture and Meridian Studies

journal homepage: www.jams-kpi.com

RESEARCH ARTICLE

A Novel Technique for Visualizing the Intralymphatic Primo Vascular System by Using Hollow Gold Nanospheres

Eric Carlson [1], Gustavo Perez-Abadia [1], Staci Adams [2], Jin Z. Zhang [2], Kyung A. Kang [3,*], Claudio Maldonado [1,4,*]

[1] *Department of Physiology and Biophysics, University of Louisville, Louisville, USA*
[2] *Department of Chemistry and Biochemistry and W. M. Keck Center for Nanoscale Optofluidics, University of California, Santa Cruz, USA*
[3] *Department of Chemical Engineering, University of Louisville, Louisville, USA*
[4] *Department of Surgery, University of Louisville, Louisville, USA*

Available online 8 October 2015

Received: Jun 4, 2015
Revised: Sep 14, 2015
Accepted: Sep 17, 2015

KEYWORDS
hollow gold nanospheres;
lymph nodes;
lymphatics;
microscopy;
optical imaging

Abstract
Until recently, the primo vascular system (PVS) has been unnoticed by most anatomists due to the small diameter and translucent features of the threadlike network. These properties make primo vessels (PVs) difficult to visualize for harvest and for further characterization. One particular PVS subtype that is located within the lymphatic vessels (LVs) is of strong interest because with a proper contrast, these long PVs can be visualized through the transparent LV wall and can be harvested to provide sufficient sample material for analysis. The most common method to visualize this PVS subtype utilizes Alcian blue as the contrast agent. This technique is effective, but tedious, and has relatively low repeatability. The purpose of this study was to develop a new technique that allows reliable visualization of the intralymphatic PVS (IL-PVS) in a user-friendly manner. The method was designed to provide

* Corresponding authors. Claudio Maldonado, 500 South Preston St., Room 1115, Department of Physiology and Biophysics, University of Louisville, Louisville, KY 40292, USA. Kyung A. Kang, Department of Chemical Engineering, J.B. Speed School of Engineering, University of Louisville, Louisville, KY 40292, USA.
E-mail: kyung.kang@louisville.edu (K.A. Kang), cjmald01@louisville.edu (C. Maldonado).

pISSN 2005-2901 eISSN 2093-8152
http://dx.doi.org/10.1016/j.jams.2015.09.003

primo vascular system;
primo vessel

optical contrast to the PVS by taking advantage of the porous nature of the PV's external wall and interstitial matrix. Turquoise-green-colored hollow gold nanospheres (HGNs) in the size range of 50—125 nm were found to provide excellent optical contrast for the IL-PVS in rats. The PVS was visualized within 10 minutes after HGN administration at a 95% success rate.

1. Introduction

In the early 1960s, Bong-Han Kim [1—3] discovered a new systemic circulatory network that he later named the Bonghan system. The system is composed of small vessels (Bonghan ducts) and nodes (Bonghan corpuscles), and each Bonghan duct contains multiple smaller ductules. According to Kim's [1—3] reports the Boghan system contained various biochemicals related to immune activities and "Sanals", cells with self-regenerating properties. Based on radioactive tracer studies performed in rabbits, Kim [1—3] believed that the system's skin network anatomically corresponds to the acupuncture meridians. Investigation on the Bonghan system was almost completely halted between1966 and 2000 for reasons not directly related to the science [4]. In the early 2000s, after reviewing Kim's findings, Kwang-sup Soh [5] restarted the research on this vessel network, and in 2010 the system was renamed the primo vascular system (PVS). Bonghan duct, ductule, corpuscle, and Sanals were renamed: primo vessel (PV), primo subvessel (subPV), primo node (PN), and primo-microcells (p-microcells), respectively.

The PVS network is systemically present in mammals in solid organs, structures of the central nervous system, skin, and inside blood and lymphatic vessels (LVs) [2,6—11]. The potential regenerative role of the PVS was initially described by Bonghan Kim [1—3], and recent reports suggest that the PVS plays a role in nonmarrow hematopoiesis and as a storage site for adult stem cells [12,13]. The PVS network is small in diameter (range, 20—50 μm) and translucent [10,14,15], making it difficult to visualize even with the aid of a microscope. No biomarkers for the PVS have been identified. Although there have been significant advances in PVS research during the past decade, characterization of the system has been progressing relatively slowly because of the difficulties in visualizing it.

The PVS inside lymphatic vessels (intralymphatic PVS; IL-PVS) has been gaining attention because this subtype affords some advantages that can facilitate the advancement of PVS research. One of these advantages is that LV walls are translucent, and because the IL-PVS can be selectively contrasted, it can be visualized through the LV wall. Another advantage is that multiple PVs running the length of various LVs can be harvested and can provide sufficient PVS material for molecular characterization. The presence of the IL-PVS has been observed in different species including rabbit, rat, and mouse [2,10,16—18]. Techniques reported for visualizing the IL-PVS include phase contrast microscopy [11], and optical microscopy with contrast agents such as fluorescent nanoparticles [16,17,19], Janus Green B [20], and Alcian blue [10,18,21,22]. The optical microscopy method using Alcian blue appears to work the best for now, but it is tedious and time-consuming [10,21,22]. When we performed rat studies using Alcian blue the success rate for visualizing the IL-PVS was $< 20\%$ (unpublished data), suggesting the need for a more reliable and simpler technique.

The main objective of this study is, therefore, to develop a new method for identifying the IL-PVS in a user-friendly way and with an acceptable repeatability. The technique was designed after carefully studying the unique microanatomical structures of the PV and its subPVs inside an LV [2,23]. One of the main characteristics of the PV is that it has pores on its external wall [23—26]. Findings from a rabbit PV study using phase contrast X-ray microscopy described that PV pores were ~0.5 mm apart along the PV wall and appeared to be oval in shape [23]. On average, the internal diameter of the pore was reported to be smaller (~1 μm) than the external diameter (2—5 μm) suggesting that lymph inflow into PVs is relatively easier than outflow [23]. As previously stated, a PV has multiple subPVs and the interstitial space between subPVs is filled with fibrous connective tissues [1]. Based on these microanatomical characteristics of the IL-PVS and LV, we have designed a method to optically contrast the IL-PVS specifically, using hollow gold nanospheres (HGNs).

Fig. 1 is a schematic diagram, illustrating an intralymphatic PV (IL-PV) and how HGNs specifically contrast the PV. Fig. 1A displays the structural characteristics of an IL-PV in an LV, with the pores on the PV wall and multiple subPVs internally. In this figure, to illustrate the concept, PNs, which normally run along the PV, are not shown. The infused nanospheres fill the LV first (Fig. 1B) and then enter the IL-PV via the pores on its wall. Properly sized HGNs inside the PV are then trapped in the fibrous interstitial space. As the lymphatic fluid clears the LV, the nanospheres generate an optical contrast for the PV (Fig. 1C).

Properly-sized HGNs fit our study purposes well because: (1) they are nontoxic, biocompatible, and chemically inert; (2) they are well dispersed in biofluid and found to not easily react with biomolecules in the lymphatic fluid; and (3) their size can be easily controlled and their color can be adjusted to generate an optical contrast against the background color of the tissue.

2. Materials and methods

2.1. Animal model and surgical procedure

Fifteen pathogen-free male and four female Sprague Dawley rats weighing 250—400 g were used in the study (Harlan Sprague Dawley, Indianapolis, IN, USA). Animals were housed two per cage in an Association for Assessment and Accreditation of Laboratory Animal Care (AAALAC)-approved vivarium. Housing conditions consisted of a 12:12-hour dark—light cycle, and the temperature was maintained at 22°C. Animals were provided with food and water *ad libitum*. All animals received humane care in compliance

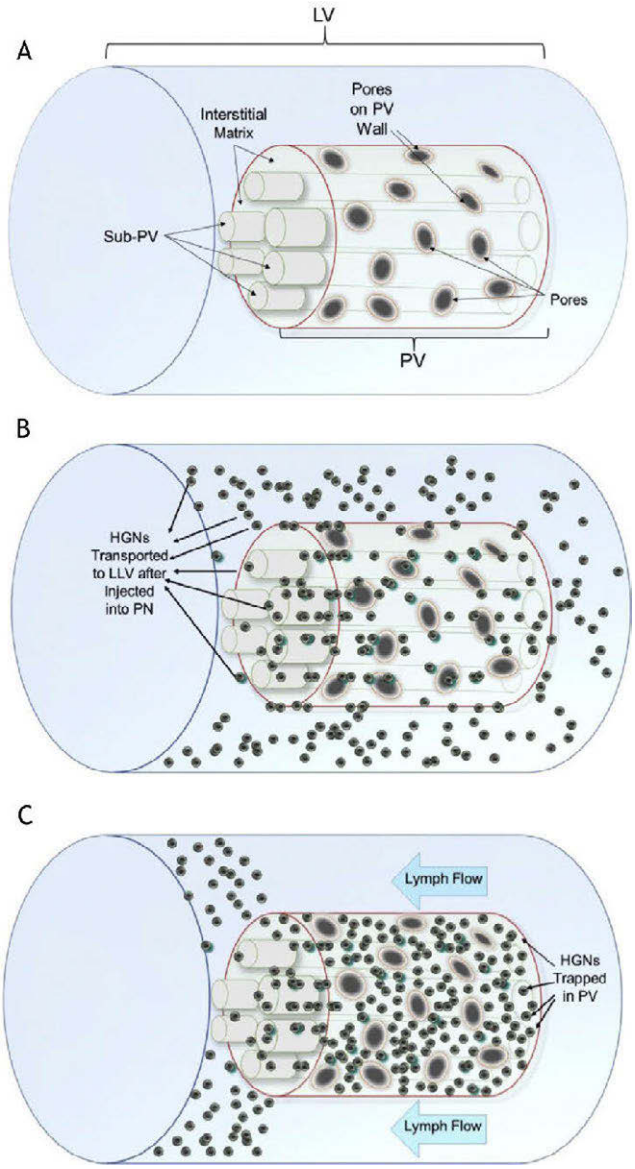

Figure 1 Postulated mechanism of how HGNs provide optical contrast to the IL-PVS. (A) Diagram of microstructures of an LV containing a PV with pores on its wall, subPVs inside the PV, and the interstitial space matrix surrounding subPVs; (B) infused HGNs fill the LV, and lymphatic fluid flow carry HGNs into the PV via its pores and are trapped in the interstitial space matrix between subPVs; (C) with time, lymphatic flow clears free HGNs from the LV and HGNs trapped in the PV provide the optical contrast. HGN = hollow gold nanospheres; IL-PVS = intralymphatic primo vascular system; LV = lymphatic vessels; PV = primo vessels; subPV = primo subvessel.

with the "Guide for the Care and Use of Laboratory Animals" prepared by the Institute of Laboratory Animal Resources and published by the National Institutes of Health (NIH Publication No. 85-23, Revised 1996). The animal protocol was approved by the guidelines established by the Institutional Animal Care and Use Committee of the University of Louisville (Louisville, KY, USA). The animal facilities at the University of Louisville are fully accredited by the AAALAC, International.

Rats were anesthetized with sodium pentobarbital (50 mg/kg body weight) administered intraperitoneally. The abdomen was shaved with electric clippers and an incision site was prepared for surgery. A midline abdominal incision ~5 cm long was made down the linea alba to the symphysis pubis. The intestines were carefully moved to the right side of the abdomen to allow visualization and access to both right and left lumbar lymphatic nodes (LLNs). A Zeiss Op-Mi6 stereomicroscope (Zeiss, Peabody, MA, USA) with variable magnification up to 40× was used during the entire experimental procedure.

2.2. HGN synthesis and preparation for infusion

HGNs were synthesized according to the method developed by the Zhang group [27—29]. Briefly, cobalt nanoparticles were synthesized first, and then gold shells were grown on their surface. Then cobalt particles were oxidized and dissolved generating HGNs. The schemes for the HGN production are described as follows:

$$2\ CoCl_2 + 4\ NaBH_4 + 9\ H_2O \rightarrow Co_2B + 4\ NaCl + 12.5\ H_2 + 3\ B(OH)_2 \quad (1)$$

$$4\ Co_2B + 3O_2 \rightarrow 8\ Co + 2\ B_2O_3 \quad (2)$$

$$3\ Co^0 + 2Au^{3+} \rightarrow 3Co^{2+} + 2Au^0 \quad (3)$$

The HGN size ranges that we selected for our study were 50—70 nm and 100—125 nm. The particle colors were turquoise and green for the 50—70 nm and 100—125 nm, respectively. Their peak absorption wavelengths were 675 nm and 800 nm, respectively. When HGNs were produced, the optical density at their respective peak was in the range of 0.35—5.0. The HGNs were then characterized by high-resolution transmission electron microscopy (HRTEM). Fig. 2 shows a high-resolution transmission electron microscopy image of HGNs. In the figure, the gold layer and the hollow space inside the particle can be clearly seen. They are spherical and the gold layer thickness is homogenous.

Prior to use for IL-PVS visualization, HGNs were concentrated 30 times by centrifugation for 30 minutes at 400 g for the particles with a diameter range of 100—125 nm, and at 1125 g for the particles 50—70 nm. After centrifugation the supernatant was carefully removed leaving an HGN pellet. The pellet was resuspended in phosphate buffered saline (PBS) to constitute a 400-μL HGN suspension and it was drawn into a 1-mL syringe ready for infusion.

2.3. Visualization and harvesting of the IL-PVS using HGNs

Rats were divided into three study groups to determine the effect of HGN size on IL-PVS visualization and also to determine whether gender was important. In Group 1 (n = 11), LLNs of male rats were injected with HGNs in a size range from 100 to 125 nm. In Group 2 (n = 4), LLNs of male rats were injected with HGNs in a size range from 50 to 70 nm. In Group 3 (n = 4), LLNs of female rats were injected with HGNs in a size range from 50 nm to 70 nm.

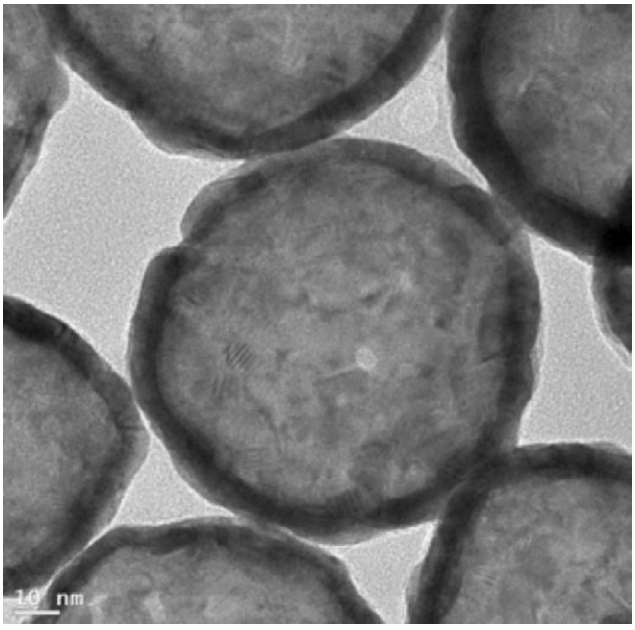

Figure 2 A high-resolution transmission electron microscopy image of HGNs. The particles are spherical and uniform in size. The gold layer is the dark gray area and the hollow inside of HGNs is clearly seen. HGN = hollow gold nanospheres.

The prepared HGN suspension (400 μL) was injected slowly at a time span of ~15 seconds into the LLNs using a 30-gauge needle. Within minutes following the infusion of the HGN suspension, abdominal fatty tissue surrounding LVs was carefully dissected to better visualize the lumen of vessels. When the HGN-contrasted PV became visible, it was carefully monitored for free movement to further confirm it as an IL-PV. To harvest a positively confirmed IL-PV, its length was first determined, and then both the LV and the intralymphatic PV were cut proximally from the LLN with a pair of microscissors and the distal end was detached with two acupuncture needles (100 μm in diameter).

2.4. Staining of IL-PV nuclei

Harvested IL-PVs were fixed in 4% paraformaldehyde solution for 20 minutes at room temperature. Samples were washed in PBS three times and placed on a glass slide. By using a PAP pen (Sigma-Aldrich, St. Louis, MO, USA), samples were encircled to create a barrier and prevent excessive spreading of reagents. One μL of 4′,6-diamidino-2-phenylindole (DAPI) from a 2.5-mg/mL stock solution (Biotium, Inc., Hayward, CA, USA), was diluted in 10 mL of PBS (1:10,000 dilution). A drop of DAPI was placed on the samples and allowed to react for 20 minutes. The samples were washed with PBS five times, and a cover slip with fluoroshield mounting medium (Sigma—Aldrich) was placed on top of the samples. Stained samples were visualized and analyzed for their fluorescence (350 nm excitation and 470 nm emission) under an Olympus FluoView1000 laser scanning confocal microscope (Olympus, Center Valley, PA, USA).

3. Results

3.1. Visualization and harvesting of the IL-PVS using HGNs

Fig. 3 shows the LLN and LV immediately after HGN injection into the LLN. Both the LLN and LV darkened after HGN infusion, but LVs remained partially translucent allowing visualization of IL-PVs soon after particle administration. Fig. 4 illustrates visualization of the IL-PVS in multiple LVs including large and small vessels (Fig. 4A). Fig. 4B shows a high magnification (40×) image of a PV inside the LV. Also, a structure with a greater diameter resembling a PN is observed along the IL-PV.

Fig. 5 demonstrates the process of IL-PVS harvest. Fig. 5A shows an IL-PV contrasted by HGNs. After determining the length of the IL-PV to be harvested, the LV and IL-PV were divided proximally to the LLN (Figs. 5A and 5B), and the distal end of the IL-PV was detached using a pair of acupuncture needles. Then, the proximal end was manipulated outside the LV (Fig. 5C) with the aid of the acupuncture needles, and the IL-PV was gently pulled out of the LV with a pair of forceps (Fig. 5D).

Table 1 summarizes our experimental study results. With the HGN method, the IL-PVS was confirmed in 18 out of 19 rats studied. HGNs for both size ranges tested, i.e., 50—70 nm and 100—125 nm, provided good optical contrast for the IL-PVS. The method produced the same results in both genders. The average time between the HGN injection and the IL-PVS to be visible was < 10 minutes. The only failure was experienced with one of the earlier cases,

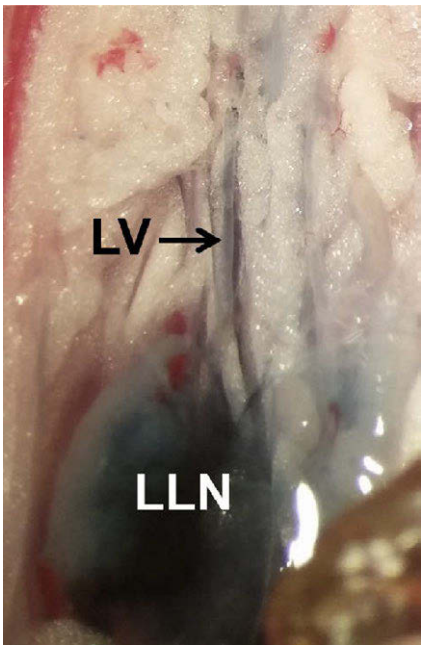

Figure 3 Appearance of a rat's LLN and LV following an injection of 50—70 nm HGNs. Notice the appearance of the LV lumen following HGN administration, it is dark with a turquoise-greenish tint, but remains translucent. HGN = hollow gold nanospheres; LLN lumbar lymphatic nodes; LV = lymphatic vessels.

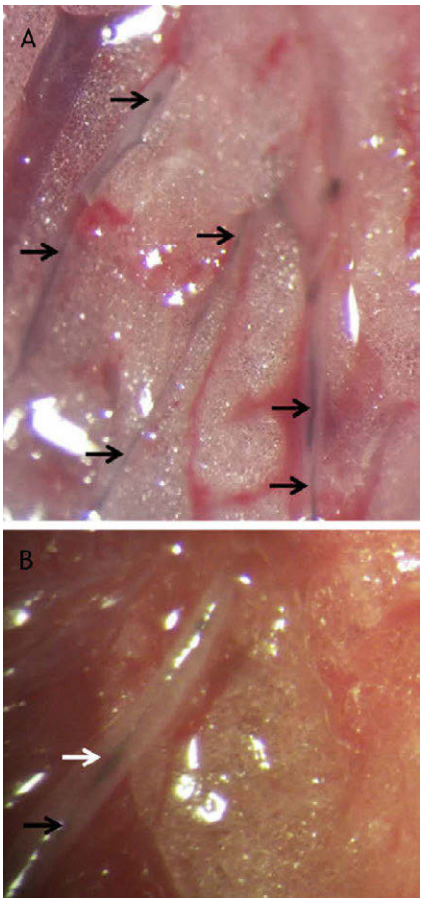

Figure 4 (A) A low magnification image (30×) of multiple LVs with IL-PVs (black arrows) in rat, contrasted by HGNs. (B) High magnification image (40×) of IL-PV (black arrow) with a greater diameter structure resembling a PN (white arrow) contrasted by HGNs. HGN = hollow gold nanospheres; IL-PV = intralymphatic primo vessels; PN = primo node.

which appeared to be caused by a faulty HGN injection. Following the HGN injection, LVs did not darken as expected, indicating that HGNs were not flowing out from the LLN into the LVs.

3.2. Staining of IL-PV nuclei

As no biomarkers unique and specific for the IL-PVS are known, the unique shape of the subPV cell nuclei serves as a surrogate method to morphologically confirm that the harvested sample is derived from the PVS. The nuclei of subPV endothelial cells are rod-shaped [1], unlike the more rounded nuclei of cells in blood and lymphatic vessels. Fig. 6 shows that the harvested IL-PV stained with DAPI has rod shaped nuclei suggesting that the sample is in fact the PVS.

4. Discussion

This feasibility investigation, as described above, was undertaken to determine whether the HNG method would serve as an efficacious, consistent, and user-friendly IL-PVS identification technique. Also, the IL-PVS was visualized using the same size HGNs in both male and female rats, indicating that the microanatomical structure of the IL-PVS is similar between genders.

During the planning stages of the project, we searched the literature and found limited information on external

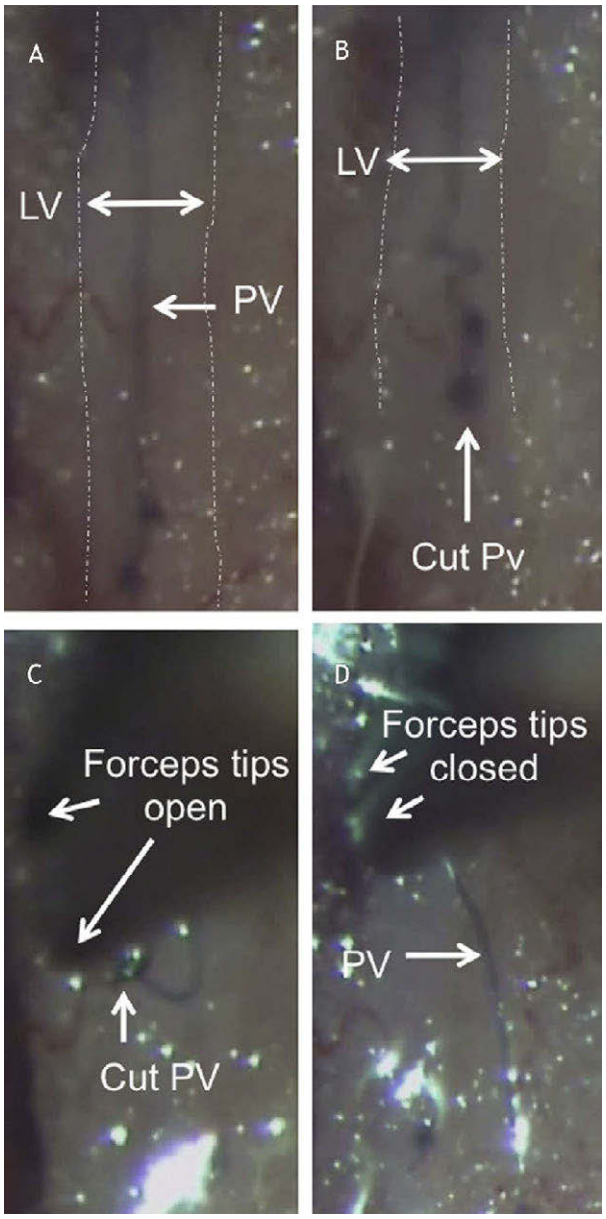

Figure 5 Sequential processes to harvest an IL-PV. (A) First, the IL-PVS was visualized by HGNs; (B) the LV and IL-PV were cut proximally to the LLN. Notice curling of the IL-PV inside the LV; (C) the distal end of the IL-PV was detached from the LV using a pair of acupuncture needles (not shown) through the LV wall; (D) the proximal end of the IL-PV was manipulated towards the outside of the cut LV vessel with the acupuncture needles, and a pair of microforceps was used to gently pull the IL-PV out of the LV. HGN = hollow gold nanospheres; IL-PV = intralymphatic primo vessel; IL-PVS = intralymphatic primo vascular system; LLN = lumbar lymphatic nodes; LV = lymphatic vessels.

Table 1 Summary of results of IL-PVS visualization in rats using HGNs.

Group No.	Gender (*n*)	HGN size (nm)	Color	No. of rats identified with IL-PVS	Time to visualize IL-PVS (min)
1	M (11)	100—125	Green	10	9.2 ± 2.6
2	M (4)	50—70	Turquoise	4	7.5 ± 2.5
3	F (4)	50—70	Turquoise	4	10.0 ± 4.5

HGN = hollow gold nanospheres; IL-PVS = intralymphatic primo vascular system.

wall PV pore dimensions. There was some data from rabbit studies on the shape and size of pores from an internal organ PV [23]. However, no detailed information was found on pore size of the fibrous matrix inside the PV. Therefore, we arbitrarily selected HGNs ranging in size from 50 to 125 nm because they are small enough to enter pores 1—2 μm in diameter. Fortunately, the size range that we selected served our study purpose well. As shown in Table 1, the IL-PVS was identified in 18 out of 19 rats.

Before the study with HGNs, we also used the Alcian blue method to visualize the IL-PVS with a low success rate. This low rate could be attributed to a lack of experience with the Alcian blue method. However, we had a 95% success rate with the HNG method, which was our first time performing it, and implies that this technique would be helpful to scientists interested in studying the IL-PVS with minimal training. The HGNs technique provided optical contrast to visualize IL-PVs in large as well as small LV branches (Fig. 4A), which was not as apparent in our Alcian blue studies (data not published). This finding suggests that the PVS appears to be present in most LVs.

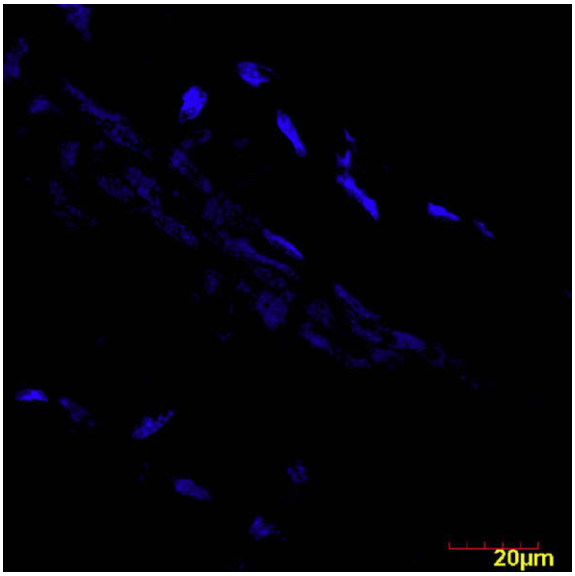

Figure 6 An image of DAPI stained rat IL-PV. The characteristic rod-shaped nuclei of the PV are clearly shown. DAPI = 4′,6-diamidino-2-phenylindole; IL-PV = intralymphatic primo vessel; PV = primo vessels.

Although many reports on the PVS have demonstrated that the system has an important role in normal physiological function, difficulties in identifying and harvesting its components has significantly delayed the advancement of PVS research. Our approach to developing an IL-PVS visualization technique, based on the microstructure of the PV, which uses properly sized HGNs with ideal optical contrast properties, provided a rapid and reliable method. Administration of HGNs to LLNs in a size range of 50—125 nm provided a turquoise to green color optical contrast that allowed us to identify the IL-PVS within 10 minutes at a 95% success rate in a rat model.

It is our hope that our new technique will assist PVS scientists to study the system more effectively, leading to additional comprehensive analyses of the PVS. We plan to refine our technique to visualize other PVS-subtypes.

Disclosure statement

The authors declare that they have no conflicts of interest and no financial interests related to the material of this manuscript.

Acknowledgments

We want to acknowledge Dr. Sathnur Pushpakumar for his assistance with DAPI staining and with confocal microscopy imaging. We would also like to thank Dr. Kyunghee Bae at the Nano Primo Research Center at the Advanced Institute of Convergence Technology, Seoul National University, Seoul, Korea for her help teaching our group how to identify the IL-PVS using Alcian Blue. J.Z.Z. is grateful to Delta Dental Health Associates and Smart Technologies for financial support on the synthesis and characterization of HGNs.

References

[1] Kim BH. On the Kyungrak System. Pyongyang, Democratic Peoples Republic of Korea: Foreign Language Publishing House; 1964.
[2] Kim BH. Kyungrak System and Theory of Sanal. Pyongyang Democratic Peoples Republic of Korea: Medical Science Press; 1965.
[3] Kim BH. Great Discovery in Biology and Medicine — Substances of Kyungrak. Pyongyang, Democratic Peoples Republic of Korea: Foreign Language Publishing House; 1962.
[4] Kang KA. Historical observations on the half-century freeze in research between the Bonghan system and the primo vascular system. *J Acupunct Meridian Stud*. 2013;6:285—292.
[5] Soh KS, Kang KA, Ryu YH. 50 years of bong-han theory and 10 years of primo vascular system. *Evid Based Complement Alternat Med*. 2013;2013:587827.
[6] Shin HS, Johng HM, Lee BC, Cho SI, Soh KS, Baik KY, et al. Feulgen reaction study of novel threadlike structures (Bonghan ducts) on the surfaces of mammalian organs. *Anat Rc B New Anat*. 2005;284:35—40.
[7] Nam MH, Lim J, Choi SH, Kim S, Soh KS. A primo vascular system underneath the superior sagittal sinus in the brain of a rabbit. *J Acupunct Meridian Stud*. 2012;5:210—217.

[8] Lee BC, Kim KW, Soh KS. Visualizing the network of Bonghan ducts in the omentum and peritoneum by using Trypan blue. *J Acupunct Meridian Stud*. 2009;2:66—70.
[9] Yoo JS, Kim MS, Ogay V, Soh KS. *In vivo* visualization of Bonghan ducts inside blood vessels of mice by using an Alcian blue staining method. *Indian J Exp Biol*. 2008;46:336—339.
[10] Lee C, Seol SK, Lee BC, Hong YK, Je JH, Soh KS. Alcian blue staining method to visualize Bonghan threads inside large caliber lymphatic vessels and x-ray microtomography to reveal their microchannels. *Lymphat Res Biol*. 2006;4:181—190.
[11] Lee BC, Soh KS. Contrast-enhancing optical method to observe a Bonghan duct floating inside a lymph vessel of a rabbit. *Lymphology*. 2008;41:178—185.
[12] Lee SJ, Park SH, Kim YI, Hwang S, Kwon PM, Han IS, et al. Adult stem cells from the hyaluronic acid-rich node and duct system differentiate into neuronal cells and repair brain injury. *Stem Cells Dev*. 2014;23:2831—2840.
[13] Hwang S, Lee SJ, Park SH, Chitteti BR, Srour EF, Cooper S, et al. Nonmarrow hematopoiesis occurs in a hyaluronic-acid-rich node and duct system in mice. *Stem Cells Dev*. 2014;23:2661—2671.
[14] Noh YI, Rho M, Yoo YM, Jung SJ, Lee SS. Isolation and morphological features of primo vessels in rabbit lymph vessels. *J Acupunct Meridian Stud*. 2012;5:201—205.
[15] Kang KA, Maldonado C, Perez-Aradia G, An P, Soh KS. Primo vascular system and its potential role in cancer metastasis. *Adv Exp Med Biol*. 2013;789:289—296.
[16] Johng HM, Yoo JS, Yoon TJ, Shin HS, Lee BC, Lee C, et al. Use of magnetic nanoparticles to visualize threadlike structures inside lymphatic vessels of rats. *Evid Based Complement Alternat Med*. 2007;4:77—82.
[17] Lee S, Ryu Y, Cha J, Lee JK, Soh KS, Kim S, et al. Primo vessel inside a lymph vessel emerging from a cancer tissue. *J Acupunct Meridian Stud*. 2012;5:206—209.
[18] Jung SJ, Bae KH, Nam MH, Kwon HM, Song YK, Soh KS. Primo vascular system floating in lymph ducts of rats. *J Acupunct Meridian Stud*. 2013;6:306—318.
[19] Lim J, Jung JH, Lee S, Su Z, Qiang Z, Cha JM, et al. Estimating the density of fluorescent nanoparticles in the primo vessels in the fourth ventricle and the spinal cord of a rat. *J Biomed Opt*. 2011;16:116010.
[20] Lee BC, Yoo JS, Baik KY, Kim KW, Soh KS. Novel threadlike structures (Bonghan ducts) inside lymphatic vessels of rabbits visualized with a Janus Green B staining method. *Anat Rc B New Anat*. 2005;286:1—7.
[21] Jung SJ, Cho SY, Bae KH, Hwang SH, Lee BC, Kim S, et al. Protocol for the observation of the primo vascular system in the lymph vessels of rabbits. *J Acupunct Meridian Stud*. 2012;5:234—240.
[22] Lee SH, Bae KH, Kim GO, Nam MH, Choi YB, Kwon HM, et al. Primo vascular system in the lymph vessel from the inguinal to the axillary nodes. *Evid Based Complement Alternat Med* 2013;2013. http://dx.doi.org/10.1155/2013/472704:1—6. Article ID 472704.
[23] Kim MS, Oh SW, Lm JH, Han SW. Phase contrast x-ray microscopy study of rabbit primo-vessels. *Appl Phys Lett*. 2010;97:213703.
[24] Yoo JS, Ayati MH, Kim HB, Zhang WB, Soh KS. Characterization of the primo-vascular system in the abdominal cavity of lung cancer mouse model and its differences from the lymphatic system. *PLoS One*. 2010;5:e9940.
[25] Lee BC, Yoo JS, Ogay V, Kim KW, Dobberstein H, Soh KS, et al. Electron microscopic study of novel threadlike structures on the surfaces of mammalian organs. *Microsc Res Tech*. 2007;70:34—43.
[26] Sung B, Kim MS, Lee BC, Yoo JS, Lee SH, Kim YJ, et al. Measurement of flow speed in the channels of novel threadlike structures on the surfaces of mammalian organs. *Naturwissenschaften*. 2008;95:117—124.
[27] Schwartzberg AM, Olson TY, Talley CE, Zhang JZ. Synthesis, characterization, and tunable optical properties of hollow gold nanospheres. *J Phys Chem B*. 2006;110:19935—19944.
[28] Schwartzberg AM, Zhang JZ. Novel optical properties and emerging applications of metal nanostructures. *J Phys Chem C*. 2008;112:10323—10337.
[29] Adams S, Thai D, Mascona X, Schwartzberg AM, Zhang JZ. Key factors affecting the reproducibility of synthesis and growth mechanism of near-infrared absorbing hollow gold nanospheres. *Chem Mater*. 2014;26:6805—6810.